Magnetization Plateaus and Sublattice Ordering in Easy-Axis Kagome Lattice Antiferromagnets

Arnab Sen,[1] Kedar Damle,[1,2] and Ashvin Vishwanath[3]

[1]*Department of Theoretical Physics, Tata Institute of Fundamental Research, Homi Bhabha Road, Mumbai 400005, India*
[2]*Physics Department, Indian Institute of Technology Bombay, Mumbai 400076, India*
[3]*Department of Physics, University of California, Berkeley, California 74720, USA*
(Received 5 July 2007; revised manuscript received 11 September 2007; published 6 March 2008)

We study kagome lattice antiferromagnets where the effects of easy-axis single-ion anisotropy (D) dominates over the Heisenberg exchange J. For $S \geq 3/2$, virtual quantum fluctuations help lift the extensive classical degeneracy. We demonstrate the presence of a one-third magnetization plateau for a broad range of magnetic fields $J^3/D^2 \lesssim B \lesssim JS$ along the easy axis. The fully equilibrated system at low temperature on this plateau develops an unusual nematic order that breaks sublattice rotation symmetry but not translation symmetry; however, extremely slow dynamics associated with this ordering is expected to lead to glassy freezing of the system on intermediate time scales.

Geometrically frustrated magnets, which are characterized by a large number of symmetry unrelated classical ground states, display a wealth of new phenomena. In contrast to their unfrustrated counterparts, in which the low temperature ordering is largely determined by classical energetics even for small spin length S, quantum effects can play a crucial role in frustrated magnets, precisely because the classical energetics fails to pick a unique state. Of particular interest are those systems in which a broad cooperative paramagnetic regime [1] at intermediate temperatures gives way at low temperature to a variety of novel ordered and liquid phases [2] arising from the quantum fluctuations of spins. Even when magnetic order is selected, the resulting patterns are often complex, and are promising candidates for realizing multiferroic properties [3].

The kagome lattice composed of corner sharing triangles is one of the most frustrated lattice arrangements possible, and one that occurs commonly in nature. Ground states of the antiferromagnetic Heisenberg model on this lattice typically involve coplanar arrangement of spins, and are extensively degenerate in the limit of classical spins [4]. Despite much work on the role of quantum fluctuations in lifting this degeneracy, several fundamental questions regarding the ground state of low spin kagome antiferromagnets (e.g., $S = 1/2, 1, 3/2 \ldots$) remain to be decisively settled [2].

In some cases however, collinear spin arrangements are preferred, for example, in the presence of strong single-ion anisotropy that leads to an easy axis. This occurs in the recently studied $Nd_3Ga_5SiO_{14}$ (NGS) compound [5,6], where Nd^{3+} (total angular momentum $\mathbf{J} = 9/2$) ions form a kagome antiferromagnet in which the common c axis is the easy axis at low temperature (below 33 K). The classical ground states of such collinear spins are also extensively degenerate. In contrast to the isotropic case, the effect of quantum fluctuations in selecting the low temperature state can be studied in a much more controlled fashion, and this is the focus of our work here.

Our results are readily stated. First, the selection mechanism depends strongly on the spin length S. Below a critical spin length $S_c = 3/2$, quantum transitions between different classical ground states dominate the degeneracy splitting. This "kinetic energy" dominated selection applies only to $S = 1$ ($S = 1/2$ does not admit a single ion anisotropy): There, a uniform spin nematic ground state was found in zero field, and a one-third magnetization ($m = 1/3$) plateau with $\sqrt{3} \times \sqrt{3}$ collinear order was obtained in the presence of a magnetic field directed along the easy axis [7].

As we show here, the situation for all $S \geq S_c = 3/2$ is entirely different. In these cases, virtual quantum transitions dominate the energetics, leading to "potential energy" differences between different classical ground states. The $m = 1/3$ plateau, which is found to exist over a broad range of fields, displays an unusual nematic order at low temperature; i.e., it spontaneously breaks sublattice rotation symmetry but not translation symmetry (or spin rotation symmetry about the field direction). Furthermore, the system exhibits slow glassy dynamics in this state as a consequence of the free energy landscape induced by the "potential energy."

In zero field, we obtain a simple characterization of the collinear states selected by virtual quantum transitions. The eventual low temperature behavior in zero field depends on further entropic effects, and poses an interesting open question that will be addressed separately [8]. These results have direct experimental relevance for the low temperature, finite field state of high spin kagome magnets with easy-axis anisotropy, such as NGS [5,6], and perhaps other collinear kagome magnets as well.

Model.—Consider a layer of kagome lattice antiferromagnet, in the limit where the easy-axis anisotropy dominates over Heisenberg exchange, with a "spin" $S \geq 3/2$:

$$H = J\sum_{\langle ij \rangle} \vec{S}_i \cdot \vec{S}_j - D\sum_i (S_i^z)^2 - B\sum_i S_i^z, \qquad (1)$$

where $J > 0$ denotes the nearest neighbor antiferromagnetic spin exchange interaction between the $S \geq 3/2$ ions, $D > 0$ is the single-ion anisotropy that picks out the common easy axis z, and B, the external magnetic field along this axis, has been scaled by the magnetic moment $g\mu_B$. Because of the frustrated nature of the exchange J, the anisotropy effects can begin to dominate and pick collinear states for not-very-large D/J. In this collinear regime, we expect an analysis based on the smallness of J/D to give reliable results.

With this in mind, we use J/D as the small parameter in a systematic perturbative approach that allows us to calculate the effective low-energy Hamiltonian and the resulting low-temperature phases. While our focus here remains the kagome case, we note parenthetically that our methods generalize readily to closely related models of triangular lattice magnets in zero magnetic field; these will be discussed separately [8].

Method.—Our analysis proceeds by splitting the Hamiltonian as $H = H_0 + \lambda H_1$, where $H_0 = J\sum_{\langle ij \rangle} S_i^z S_j^z - D\sum_i (S_i^z)^2 - B\sum_i S_i^z$ and $H_1 = \frac{1}{2}\sum_{\langle ij \rangle}(S_i^+ S_j^- + \text{H.c.})$. Here $S_i^{\pm} = S_i^x \pm iS_i^y$, and λ is introduced as a bookkeeping device (λ is set to one at the end of the calculation). In each case discussed below, we begin by using standard degenerate perturbation theory [9] in λ to obtain the low-energy effective Hamiltonian that encodes the "slow" dynamics induced by the H_1 term within the ground state manifold of H_0. Terms in this expansion are naturally organized according to the power (n_λ) of λ they carry, and by the number (n_b) of different bonds on which constituents of H_1 act.

As it is possible to obtain a precise characterization of the pairs (n_λ, n_b) that contribute to leading orders in the physical expansion parameter J/D, this procedure leads us directly to the physical low-energy effective Hamiltonian at leading orders in J/D. (Reference [10] employed a closely related procedure for collinear states of the pyrochlore antiferromagnet in a field, but without anisotropy, and our calculation is better controlled due to the presence of anisotropy.)

The kagome magnet at $m = 1/3$: We begin by considering values of field such that the ground state manifold of H_0 has magnetization $m = 1/3$ and is characterized by a 2:1 constraint that requires two spins in each triangle to be maximally polarized along the field, and one, minority, spin in each triangle to be maximally polarized antiparallel to the field. While the Zeeman energy gap that drives the formation of this magnetization plateau is largest for $B \sim 2JS$, we will argue later that the plateau extends down to a relatively small onset field that scales as $B_{\text{onset}} \sim J^3/D^2$.

A convenient way to represent the ensemble of $m = 1/3$ states [11] is to encode the presence of a minority spin by

placing a dimer on the corresponding bond of the underlying honeycomb lattice [see Fig. 1(b)]. The low temperature physics on the plateau is then determined by the leading order effective Hamiltonian that acts within this dimer subspace.

Because of the strong 2:1 constraint, the first term (for any $S \geq 3/2$) that breaks degeneracy of states in the dimer subspace is a diagonal (potential energy) term that occurs at order J^6/D^5; this term arises from $n_b = 6$ $n_\lambda = 6$ processes in the Van Vleck expansion in which the six bonds on which H_1 acts form a hexagonal loop. In contrast, the leading off-diagonal term, that corresponds to changing the state of a flippable hexagon (with alternating $\pm S$ values of S_z around the hexagon) by reversing all spins on it, arises at order J^{6S-2}/D^{6S-3} (with $n_b = 3$, $n_\lambda = 6S$).

A careful evaluation of these contributions for $S = 3/2$ yields the effective Hamiltonian:

$$\mathcal{H}_{m=1/3} = \sum_{\bigcirc}\left(\frac{c_1 J^6}{6D^5}|\bigcirc_1\rangle\langle\bigcirc_1| - \frac{c_2 J^7}{D^6}(|\bigcirc_{3A}\rangle\langle\bigcirc_{3B}| + \text{H.c.})\right),$$

where $\bigcirc_m$ ($m = 0, 1, 2, 3$) denote hexagonal plaquettes with m dimers and $\bigcirc_{3A}$, $\bigcirc_{3B}$ represent the two flippable dimer configurations with three dimers on a hexagonal plaquette. The values of the coefficients are $c_1 = \frac{2187}{16\,384} \approx 0.1335$ and $c_2 = \frac{27}{8192} \approx 3.3 \times 10^{-3}$. Thus, the off-diagonal term of $\mathcal{H}_{m=1/3}$ is negligible compared to the diagonal part for $S = 3/2$. From the foregoing analysis, it is also clear that its magnitude decreases with S, and we have therefore not calculated the off-diagonal coefficient for $S > 3/2$. The potential energy $V(S) \equiv c_1(S)J^6/6D^5$ has however been calculated for general S, and the result is $V(S) = (2S)^6 J^6/1024(2S-1)^5 D^5$.

As an independent check on this result, we use the semiclassical large-S expansion procedure of Ref. [12] and directly calculate the semiclassical effective Hamiltonian in this large-S limit: The leading $\mathcal{O}(J^6/D^5)$ term obtained by expanding the semiclassical result in powers of J/D agrees precisely with the large-S limit of the perturbative result obtained above for arbitrary S.
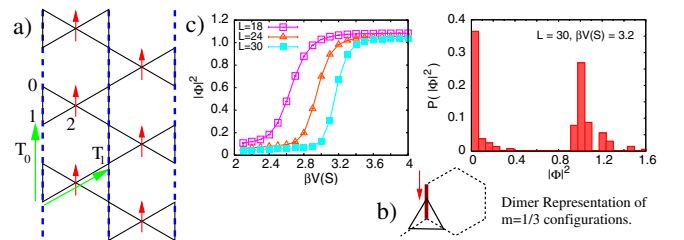

FIG. 1 (color online). (a) (Sublattice) rotation symmetry breaking on the $m = 1/3$ plateau: Dotted lines denote alternating arrangement of spins with average moment zero; up arrows correspond to $S_z = +S$. (c) First-order transition to ordered state.

The low temperature physics is thus well described by a classical dimer model with weights associated with the potential energy term in the effective Hamiltonian. Furthermore, this classical potential energy is minimized by any configuration with no hexagon having precisely one dimer on it. As there are a large number of such configurations, a more detailed analysis is needed to elucidate the nature of the low temperature state. To this end, we have employed a generalization [8] of the procedure of Refs. [13,14] to efficiently simulate an interacting classical dimer model with this potential energy term—our algorithm employs nonlocal loop updates but preserves detailed balance in order to generate the correct equilibrium Gibbs distribution at temperature T.

As the temperature is lowered to below $T_c \approx 0.23V(S)$ (obtained by extrapolating the finite L data in Fig. 1), we find that the system undergoes a transition to a state with (sublattice) rotation symmetry breaking as shown in Fig. 1(a): In this simplest schematic of the ordered state, one spontaneously chosen sublattice of spins acquires the maximal polarization $+S$ along the field. In order to satisfy the strong 2:1 constraint on each triangle, the spin moments on the other two sublattice sites then alternate $+S, -S, \ldots$ in one of the two possible alternating arrangements along a stripe. (A very similar ordering was suggested earlier for an isotropic kagome magnet in the semiclassical limit [15].) This ordering can be conveniently characterized using the sublattice order parameter $\Phi = \sum_p m_p e^{2p\pi i/3}$, where m_p denotes the sublattice magnetization of the pth sublattice [Fig. 1(a)]. The two peak structure in the histogram of $|\Phi|^2$ at T_c provides evidence for the first-order nature of the transition.

As each stripe can be in one of two possible alternating states, its internal state can be represented by an (Ising) pseudospin variable σ. Are these σ ordered in any manner, or do they fluctuate over time? The absence of any nonzero wave vector Bragg peaks in the numerically measured static structure factor of physical spins rules out any $\mathbf{q} \neq 0$ order. Furthermore, the low temperature value of $|\Phi|^2$ is, within error bars, exactly what one would expect if each stripe fluctuated between its two allowed alternating states (ruling out $\mathbf{q} = 0$ order for the pseudospins). Additional confirmation also comes from the statistics of different types of hexagons with precisely two dimers on them (not shown).

This throws up a point of general interest: Although the fully equilibrated system only breaks rotation symmetry by forming disordered stripes, this equilibration is achieved in our numerics because the algorithm incorporates nonlocal loop updates that can flip a macroscopic number of spins in one move. In the experimental system, the dynamics is of course purely local. Such local spin flips cost significant potential energy, and the system needs to change the internal state of an entire stripe to avoid this potential energy penalty. Systems with very similar potential energy

landscapes have been the subject of earlier studies which demonstrate that the time scale for changing the internal state of a stripe diverges rapidly with system size if the dynamics is local [16]. It is thus clear that the low temperature phase displays glassy freezing of the stripes.

We have also numerically studied the behavior of the system for $T_c \lesssim T$ with purely local two-spin exchange dynamics satisfying detailed balance, and monitored the temperature dependence of the single-spin autocorrelation function for a range of moderately large values for the ratio $JS^2/V(S)$. In these simulations, the magnetic field B is fixed to its nominally optimal value $B = 2JS$ which places the system close to the center of the $m = 1/3$ plateau; however, we emphasize that the ratio $JS^2/V(S)$ is kept finite as we wish to explore the higher temperature dynamics, and configurations outside the "dimer subspace" are allowed but exponentially unlikely (as opposed to forbidden). We find that the single-spin autocorrelation time τ increases very rapidly as we lower the temperature. Indeed, $\tau(T)$ can be fit well by an activated functional form of the Vogel-Fulcher type $\tau(T) = \exp(\Delta/(T - T_f(L)))$ (Fig. 2), thus extending further the analogy to other models of glass formers [16]. In our fits, the freezing temperature $T_f(L)$ drifts somewhat with linear size L, but its extrapolated $L \rightarrow \infty$ value is within 10% of the equilibrium T_c obtained earlier, while the barrier energy scale Δ shows no L dependence.

We thus conclude that while the fully equilibrated system only breaks sublattice rotation symmetry but not lattice translation symmetry, slow glassy dynamics that sets in as the temperature is lowered through T_c forces the system into a glassy state in which the stripe pseudospins also freeze in a random pattern, thereby breaking lattice translation symmetry in a random manner. What would be a good experimental signature of this behavior? Clearly, it is not appropriate to focus on elastic Bragg peaks within the first Brillouin zone, as neither the fully equilibrated sublattice ordered state nor the metastable glassy state lead to such a Bragg peak. However, we note that the sublattice order parameter that indicates the breaking of rotation symmetry can be reconstructed by taking suitable linear combinations of the measured spin structure factor close to wave vectors with components $(0, 0)$ $(0, 2\pi/a)$, $(2\pi/a, 0)$,
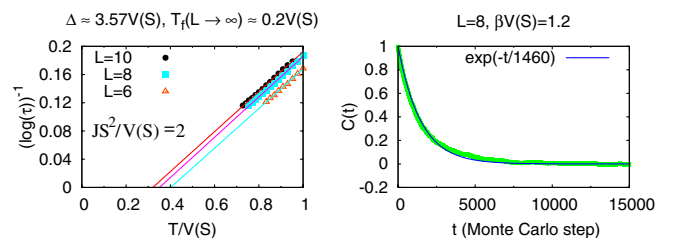
FIG. 2 (color online). Data for single-spin autocorrelation time τ fit to the Vogel-Fulcher form $(\log(\tau))^{-1} = (T - T_f)/\Delta$; the intercept on the x axis yields T_f, while the slope gives Δ^{-1}.
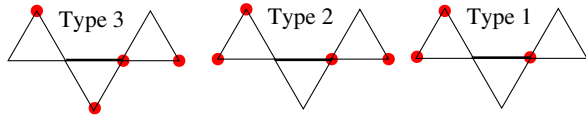
FIG. 3 (color online). The three types of unfrustrated bonds; presence (absence) of red dots represents $S_z = +S$ ($S_z = -S$).

and $(2\pi/a, 2\pi/a)$ along T_0 and T_1 [Fig. 1(a)], and this provides a possible experimental probe of sublattice symmetry breaking, that is independent of more subtle questions regarding the freezing of the stripe pseudospins.

The kagome magnet in zero field.—To understand how the onset field of the $m = 1/3$ plateau scales with J/D and S, we need to first characterize the collinear states selected by analogous potential energy effects in zero field. We begin by noting that at large D and $B = 0$, the ground states of H_0 are obtained by requiring all spins to have polarization $\pm S$ along the z axis, and allowing only one frustrated bond (pair of nearest neighbor parallel spins) per triangle.

This macroscopic degeneracy is broken by the effect of real and virtual quantum transitions. A perturbative analysis in J/D again allows us to derive a leading order effective Hamiltonian that acts within this degenerate subspace and encodes these effects:

$$\mathcal{H}_{B=0} = -W \sum_{\mathcal{B}} (2|3\mathcal{B}\rangle\langle 3\mathcal{B}| + |2\mathcal{B}\rangle\langle 2\mathcal{B}| + 0|1\mathcal{B}\rangle\langle 1\mathcal{B}|)$$
$$+ t \sum_{\mathcal{B}} (|3\mathcal{B}\rangle\langle 3\mathcal{B}'| + \text{H.c.}), \qquad (2)$$

where the sum extends over unfrustrated bonds $\mathcal{B}$. For $S = 3/2$ we find $W = \frac{27J^3}{64D^2}$, $t = \frac{9J^3}{32D^2}$, $|M\mathcal{B}\rangle$ represent unfrustrated bonds with local environment of type M (Fig. 3), and $|3\mathcal{B}\rangle$ and $|3\mathcal{B}'\rangle$ in the second (off-diagonal) term are related to each other by a spin-exchange between the antiparallel spins connected by the flippable (i.e., type-3) bond $\mathcal{B}$. More generally, for $S > 3/2$, the t term is negligible while $W(S) = \frac{S^3 J^3}{2D^2(2S-1)^2}$.

Constraints provided by the kagome geometry allow us to prove that the potential energy term W is minimized by a class of collinear configurations in which no spin is the minority spin of both triangles to which it belongs [8], and demonstrate that this class of configurations has macroscopic entropy [8].

More importantly for our purposes here, this zero field ensemble is stable to small magnetic fields since the defining constraint on minority spins does not fix the average magnetization. When the field is increased further beyond $B \sim J^3/D^2$, the $\mathcal{O}(BS)$ Zeeman energy gain of the $m = 1/3$ ensemble (defined by the 2:1 constraint) will begin to dominate over the $\mathcal{O}(J^3 S/D^2)$ potential energy gain of the zero field ensemble defined by the constraint on minority spins, and this will trigger the onset of the $m = 1/3$ plateau. Thus, the onset field will scale as $B_{\text{onset}} \sim J^3/D^2$. Since this onset field does not scale with S (and can be quite small for even moderate values of D/J), we conclude that the predicted magnetization plateau state is likely to fall well within the field regime accessible to experiment even for large S.

Discussion.—We have thus predicted an unusual sublattice ordered $m = 1/3$ magnetization plateau state with slow glassy dynamics at low temperature in pure $S \geq 3/2$ kagome antiferromagnets with strong easy-axis anisotropy. We have also provided a simple characterization of the collinear states that are selected in zero external field by an effective potential energy generated by virtual quantum fluctuations. Our results are expected to provide an excellent starting point for understanding the very low temperature physics of the kagome antiferromagnet NGS, although more work may be needed, particularly in the zero field case, to understand the effects of spatial distortion and subdominant in-plane anisotropies [5]. We hope our results provide impetus for experiments on other easy-axis kagome antiferromagnets, especially members of the large family of materials [5] that have the $Ca_3Ga_2Ge_4O_{14}$ crystal structure of NGS.

[1] R. Moessner, Can. J. Phys. **79**, 1283 (2001).
[2] G. Misguich and C. Lhuillier, in *Frustrated Spin Systems*, edited by H. T. Diepp (World Scientific, Singapore, 2005).
[3] S.-W. Cheong and M. Mostovoy, Nat. Mater. **6**, 13 (2007).
[4] D. A. Huse and A. D. Rutenberg, Phys. Rev. B **45**, R7536 (1992).
[5] P. Bordet *et al.*, J. Phys. Condens. Matter **18**, 5147 (2006).
[6] J. Robert *et al.*, Phys. Rev. Lett. **96**, 197205 (2006); **97**, 259901 (2006).
[7] K. Damle and T. Senthil, Phys. Rev. Lett. **97**, 067202 (2006).
[8] A. Sen *et al.* (to be published).
[9] H. Primas, Rev. Mod. Phys. **35**, 710 (1963).
[10] D. Bergman, R. Shindou, G. Fiete, and L. Balents, Phys. Rev. B **75**, 094403 (2007).
[11] R. Moessner and S. L. Sondhi, Phys. Rev. B **68**, 064411 (2003).
[12] U. Hizi and C. Henley, Phys. Rev. B **73**, 054403 (2006).
[13] A. W. Sandvik and R. Moessner, Phys. Rev. B **73**, 144504 (2006).
[14] F. Alet *et al.*, Phys. Rev. B **94**, 235702 (2005).
[15] S. R. Hassan and R. Moessner, Phys. Rev. B **73**, 094443 (2006).
[16] D. Das, J. Kondev, and B. Chakraborty, Europhys. Lett. **61**, 506 (2003).